IEEE Transactions on Nuclear Science, Vol. NS-28, No. 3, June 1981

END MAGNET DESIGN FOR THE NBS-LASL CW MICROTRON*

Philip H. Debenham
National Bureau of Standards
Washington, D.C. 20234

Introduction

The National Bureau of Standards and Los Alamos Scientific Laboratory are engaged in a joint research project with a goal of developing the technology necessary to build a high-current, 1-2 GeV, continuous wave (CW) electron accelerator using beam recirculation.[1] An important part of the project is the construction of a 185 MeV demonstration racetrack microtron (RTM), as shown in figure 1. Beam quality and ease of operation in an RTM are critically dependent on the properties of the end magnets. Furthermore, the overall cost of a 1-2 GeV microtron is expected to be dominated by the end magnets.[2] For these reasons it was desired to design end magnets for the demonstration RTM which meet the performance requirements at the least cost. A novel and economic magnet design has been developed which has a calculated field uniformity of better than two parts in 10^4. The design incorporates a Purcell filter into a half picture frame magnet and provides a 25% reduction in weight from an equivalent C-magnet.

Requirements on RTM End Magnets

Field Strength and Uniformity

On successive passes through an RTM, the beam must be returned to the accelerating section at nearly the same resonant phase, ϕ_R, of the RF field. This resonance condition can be written[3]

$$(2\pi/c)\Delta T = \nu\lambda B. \qquad (1)$$

Here, ΔT is the energy gain per pass, λ is the RF wavelength, ν is the harmonic number (the difference between successive orbit circumferences, in RF wavelengths), and B is the end-magnet field strength. One goal of the NBS-LASL project is to study the dependence of the beam blowup phenomenon on the accelerating gradient. The design range of ΔT is between 9.6 and 14.4 MeV per pass, which requires a range of end magnet field strengths between 0.8 and 1.2 Tesla.

The uniformity of the end magnet field determines the phase error, $\Delta\phi$, with which the beam is returned to the accelerating section. The phase acceptance of the NBS-LASL RTM is approximately 18°. We specify a full-width maximum phase error of 2°, which imposes a requirement on the field uniformity, $\Delta B/B$, of $\pm 2\times10^{-4}$ or better, averaged over any pass through the end magnets, over the operating range of 0.8 to 1.2 Tesla.

Fringe Fields

The end magnet fringe fields must be treated carefully because of the unwanted and potentially very strong defocussing which they can provide in the direction perpendicular to the magnet midplane.[4] It is undesirable because in general an RTM requires relatively weak transverse focussing. The NBS-LASL RTM is designed for an overall transverse focal length per turn of 1/2 orbit circumference (12.5 m) or more. This corresponds to a transverse betatron tune of 90° per turn or less. Yet the focal length of a normal fringe field such as that in figure 2a is only 15 cm on the first turn. We use active field clamps to produce a Babić-Sedlaček (BS) fringe field[5], as shown in figure 2b, which is adjusted for a large focal length. Adjustable transverse focussing is provided by quadrupole doublets on the return lines.

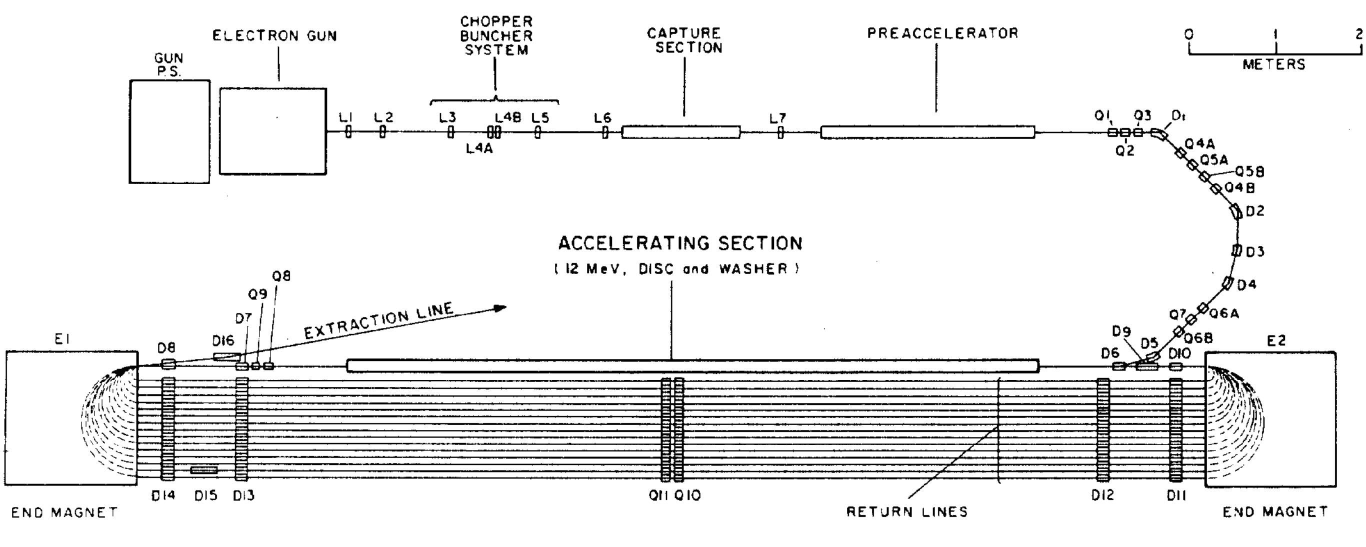

Figure 1 Plan view of the NBS-LASL RTM. A 5 MeV electron beam from the preaccelerator is recirculated through the accelerating section 15 times to a final energy of 185 MeV.

*Work supported in part by the Division of Nuclear Physics, US Department of Energy.

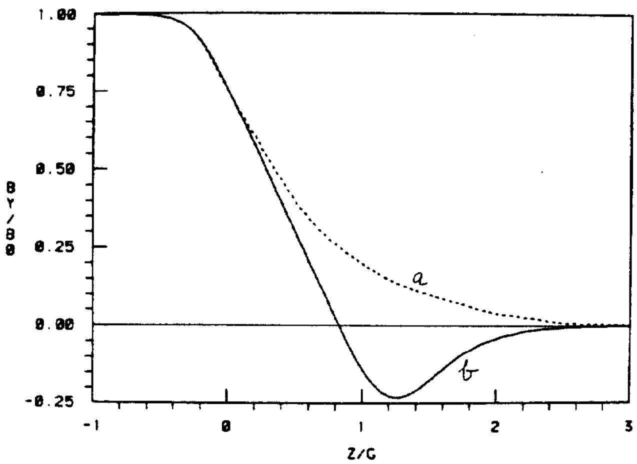

Figure 2 Fringe fields: (a) normal and (b) Babić-Sedlaček.

End Magnet Design

The fundamental problem in end magnet design is that the required field uniformity is difficult to achieve economically for the large ratio of gap depth to height typical of an end magnet. Two geometries are appropriate, as illustrated in figure 3: the C-magnet and the half picture-frame (HPF) magnet. Both designs are two-dimensional and can provide a magnetic field independent of orbit number, an important feature for an end magnet. C-magnets have been used in several racetrack microtrons.[3,6] With field-homogenizing gaps (Purcell filters),[7] a C-magnet can provide adequate field uniformity. However, the full gap depth is not useful due to the nonuniform field near the interior pole edge. The HPF magnet is more economic of iron, as virtually the entire gap depth is useful, and in the present case offers a 25% savings in weight over a C-magnet. The HPF magnet, however, has no homogenizing gap and is limited in field uniformity. We have performed magnetic field calculations using TRIM[8] for an HPF design. The calculations show a systematic field variation of three parts in 10^3 with distance into the gap. Non-uniformity in the field is manifested in the non-zero angle, θ, of the field lines in the steel-air interface. This is shown in figure 4.

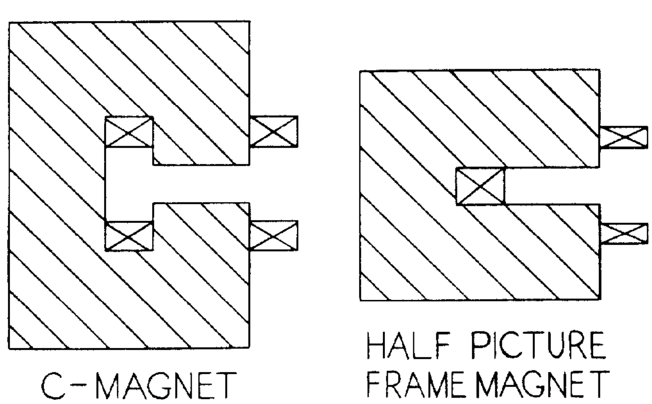

Figure 3 End magnet profiles.

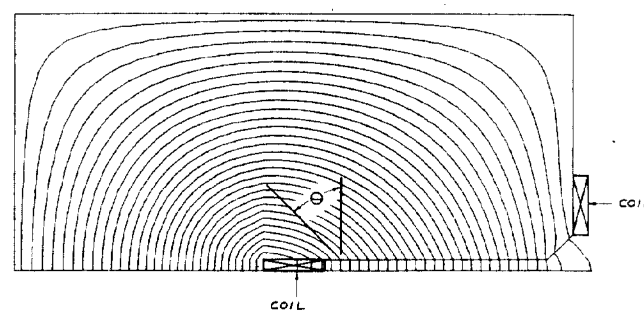

Figure 4 Calculated magnetic flux in an HPF magnet of annealed 1010 steel. The magnet is symmetric about the lower edge. Air gap flux density is 1 Tesla.

We have developed a hybrid design, shown in figure 5, which incorporates a homogenizing gap into an HPF magnet. In this design, the pole thickness is half the coil width, w. The width, b, of the inclined homogenizing gap is given by the formula

$$b = 2ag(h + \ell)/w(g - a). \qquad (2)$$

This sets the field line angle, θ, to zero at the interior of the air gap.

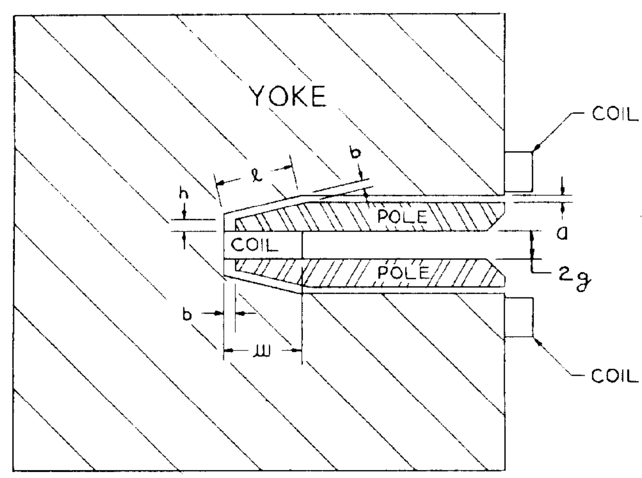

Figure 5 Hybrid HPF magnet with separate pole pieces and homogenizing gaps, width a and b.

In a full picture-frame magnet, the proper choice of the inclined homogenizing gap width, b, will homogenize the field throught the main gap. Because of the reduced symmetry in an HPF magnet, an additional design parameter is required to equalize the field intensity in the main and homogenizing gaps.[9] In our design for the NBS-LASL RTM end magnet, shown in figure 6, this is provided by a shim in the open end of the homogenizing gap. Notice that $\theta = 0$ in the pole across the entire gap depth in figure 6. The calculated midplane field, shown in figure 7, is uniform to two parts in 10^4 for field values in the operating range of 0.8 Tesla to 1.2 Tesla.

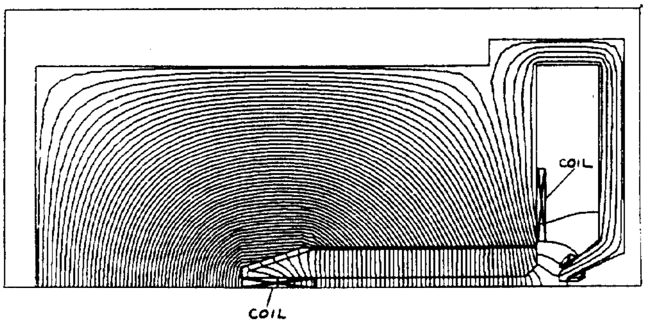

Figure 6 Calculated magnetic flux in the end magnet. 1 Tesla in air gap.

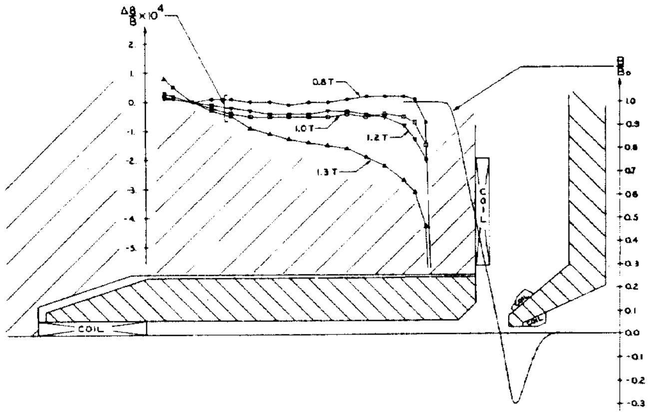

Figure 7 Calculated field on end-magnet midplane.

Active field clamps with reverse-field coils produce the non-focussing fringe field shown in figure 7. The main magnet yoke is used to return flux from the field clamps. This preserves the two-dimensional nature of the design and provides a clamp for the flux produced by the main coil return. Ray-tracing calculations using program PTRACE[10] were performed to adjust the focal length of the calculated fringe field profile to a large value. The adjusted profile was used in subsequent calculations in which beam of the expected emittance was ray-traced through the entire RTM. The purpose of these calculations was to evaluate any increase in emittance caused by the end magnet fringe fields. No significant increase was found.

The design of the NBS-LASL RTM end magnets is shown in figure 8, and some pertinent parameters are given in table 1. The gap is large (60 mm) relative to the beam diameter ($\leq$ 6 mm) to allow space for an independent vacuum chamber and corrective windings, to reduce the effect of gap variation on field homogeneity, and to produce the desired fringe field slope. Spacers are used to maintain the gap in the presence of magnetic forces. Inaccuracies in fabrication and inhomogeneities in the iron are expected to cause local field inhomogeneities of about one part in 10^3. After field mapping, such inhomogeneities will if necessary be reduced by an order of magnitude using low-power, printed-circuit-board surface windings.

Acknowledgements

Discussions with Klaus Halbach were invaluable in developing a rough idea into a working design. Eric Lindstrom did the beam optics calculations and gave timely assistance in the preparation of this paper.

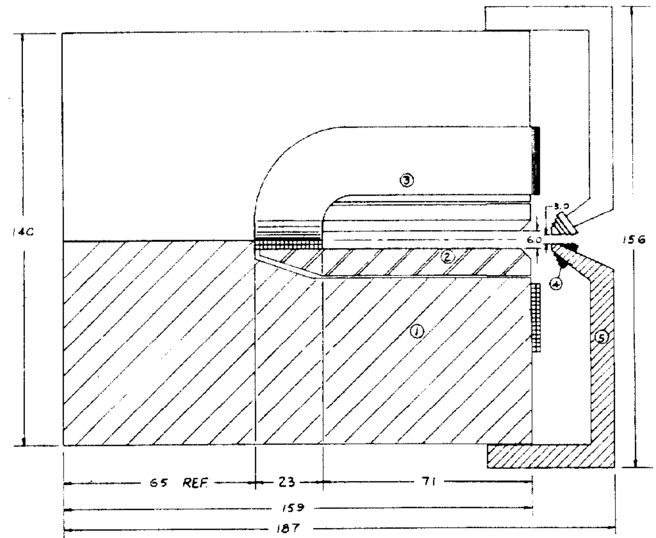

Figure 8 Side view/section of end magnet. Parts are: (1) yoke, (2) pole, (3) main coil, (4) reversing coil, and (5) field clamp. Dimensions in cm. Width perpendicular to this view is 158 cm, resulting in an approximately cubic magnet.

Table 1. End Magnet Parameters at 1 Tesla

Gap dimensions	(cm)	6x71x158
Mass of steel	(kg)	29000
Mass of copper	(kg)	420
Main coil		
Turns		64
NI	(A-turns)	58000
Power	(kW)	42
Current density	(A/cm^2)	706
Reversing coil		
NI	(A-turns)	7200

References

1. S. Penner et al., IEEE Transactions on Nuclear Science NS-28, 1526 (April 1981).
2. Y. Cho et al., "Study of a National 2-GeV Continuous Beam Electron Accelerator," ANL-PHY-79-2, Rev. 1 (August 1980).
3. H. Herminghaus et al., Nuclear Instruments and Methods 138, 1 (1978).
4. H.A. Enge, Review of Scientific Instruments 35, 278 (1964).
5. H. Babić and M. Sedlaček, Nuclear Instruments and Methods 56, 170 (1967).
6. L.M. Young, IEEE Transactions on Nuclear Science NS-20, 81 (June 1973).
7. H.A. Enge, Nuclear Instruments and Methods 28, 119 (1964).
8. A.M. Winslow, Journal of Computational Physics 2, 149 (1967).
9. K. Halbach, private communication.
10. K.H. Kaiser, private communication.